(Presented at the Conference on the Optical Properties of Ions in Crystals, Baltimore, Maryland, September 12 - 14, 1966.)

# EXCITON-MAGNON EFFECTS IN THE OPTICAL SPECTRUM OF $MnF_2$*

by

R. L. Greene and D. D. Sell†

Department of Physics

Stanford University, Stanford, California

and

R. M. White‡

Department of Physics

University of California, Berkeley, California



* Work at Stanford supported in part by the National Aeronautics and Space Administration under Grant NsG 331 and in part by the Advanced Research Projects Agency through the Stanford Materials Research Center.

† NSF Predoctoral Fellow 1965-66.

‡ Present address, Department of Physics, Stanford University.

# I. INTRODUCTION

The optical properties of magnetic materials have been studied with renewed interest during the past year. This has been due, in part, to the identification of exciton-magnon absorption (spin wave sidebands) in the visible spectrum of $MnF_2$,[1] and two magnon absorption in the infrared spectrum of $FeF_2$.[2] In this paper we discuss some of the visible absorption and fluorescence properties of antiferromagnetic $MnF_2$. In particular we consider only the sharp transitions involving the ground $\left({}^6A_{1g}\right)$ and first $\left[{}^4T_{1g}\left({}^4G\right)\right]$ excited states of the manganese ion.

Our experiments indicate that the absorption spectrum is an intrinsic property of the pure crystal, whereas the fluorescence is caused by impurities. Therefore, we consider these separately. We treat the absorption in terms of excitons and magnons. From the symmetry of the excitons and magnons, group theoretical selection rules can be found for the magnon sidebands. An explicit treatment of the interaction yields the same selection rules and shows that the exciton and magnon are generated on opposite sublattices. The emission is discussed from a single-ion viewpoint. A simple model is discussed which describes the general properties of the emission spectrum. In this case it is found that the sidebands result from an excited state and magnon on the same sublattice.



## II. ABSORPTION

Since the absorption spectrum is a property of the pure crystal, any theory we use to describe it should treat the excited states of the crystal as excitons. We have done this using the theory developed for excitons in molecular crystals. The details of this formalism have been published elsewhere;[3] here we wish to present only a few of the most pertinent results.

In general, two characteristics of excitons are important. They couple ions at different sites in the unit cell, and they have an energy and symmetry which depend on their wave vector $\underset{\sim}{k}$. In $MnF_2$ there are two sites (one on each sublattice) per unit cell which are degenerate in the absence of external perturbations. One might assume that intersublattice coupling will lift this degeneracy (Davydov splitting). However, since the transitions are spin forbidden this coupling is much smaller than the intrasublattice coupling and no Davydov splitting is expected. This is confirmed experimentally. This small coupling also allows the pure electronic transitions ($\underset{\sim}{k} = 0$) to be treated by the usual single-ion model.

The sidebands cannot be described by a single-ion model since they correspond to the excitation of an exciton and magnon with nonzero $\underset{\sim}{k}$. Thus the dispersion and symmetry of the excitons will be important. The sideband absorption is proportional to the magnon-exciton density of states weighted by the square of a wave-vector dependent interaction

matrix element. The high-frequency portion of the unweighted magnon density of states is shown in Fig. 1. The critical points indicated refer to the symmetry points of the Brillouin zone (illustrated in the left-hand corner). The symmetry of the excitons and magnons at the various points in the Brillouin zone will determine which critical points are actually allowed by the weighting factor. These selection rules can be found group theoretically, quite independent of the particular interaction responsible for the sideband process.

We consider the transition matrix element

$$\langle E^1_{\underset{\sim}{k}}, M^2_{-\underset{\sim}{k}} | \underset{\sim}{P}^{eff} | G \rangle \quad , \qquad (1)$$

where the final state has an exciton and magnon on opposite sublattices. We shall show later that this is the only type of exciton-magnon final state which can contribute to a sideband absorption. Here $\underset{\sim}{P}^{eff}$ is the effective dipole moment which allows the transition and $|G\rangle$ is the crystal ground state. From the work of Dimmock and Wheeler[4] we find that for the magnetic space group $P_{nnm}$ the magnons transform like the irreducible representations $\Gamma_3^+ + \Gamma_4^+$. The x , y , z components of $\underset{\sim}{P}^{eff}$ transform like $\Gamma_3^-$ , $\Gamma_4^-$ and $\Gamma_2^-$ , respectively. The pure exciton transition is magnetic dipole and appears in $\pi_{mag}$ ($\mathcal{H} \parallel c$) polarization. This implies that the exciton transforms like $S_z$ or the $\Gamma_2^+$ irreducible representation. The irreducible representations at other points in the Brillouin zone must be compatible with these. From the compatibility tables and the transformation properties of the excitons and magnons we find that the magnon transforms like $X_2$ , $M_3^+$ , $M_4^+$ , $A_2$ , $Z_2$ , $R_1^+$ and the exciton

transforms like $X_1$ , $M_1^+$ , $M_2^+$ , $A_1$ , $Z_1$ , $R_1^+$ . Once we know these transformation properties it is a simple matter to apply the prescription of Lax and Hopfield.[5] We find that in $\pi$ polarization only the X critical point contributes and in $\sigma$ polarization only Z and A contribute.[6] This can be compared with the two-magnon absorption where A contributes to $\pi$ and X to $\sigma$ polarization.[7] These results are in reasonable agreement with experiment.[1] However, since the exciton is derived from the complex $^4T_{1g}$ single ion state and its detailed dispersion is not known, the profiles of the sidebands cannot be fit quantitatively. In particular, just as in the two-magnon case, the $\pi$ spectrum appears somewhat broadened and shifted in frequency. This may be due to the fact that the interaction may extend beyond nearest neighbors or it may reflect the presence of phonons.

To actually find the transition moment which has the above properties it is necessary to consider a particular form for the interaction. Two theories[2,8] have been proposed. For $MnF_2$ the theory of Tanabe, Moriya, and Sugano[8] seems to be experimentally confirmed. They consider a second-order process involving nondiagonal exchange which can be written as

$$\underset{\sim}{M} = \sum_U \frac{\langle F|V|U\rangle \langle U|\underset{\sim}{P}|G\rangle}{E_G - E_U} + \left(\begin{array}{c}\text{term with } V \text{ and } \underset{\sim}{P} \\ \text{interchanged}\end{array}\right) \quad .(2)$$

Here $|F\rangle$ is the final exciton-magnon state, $|U\rangle$ is an odd intermediate state, V is the sum of all the two-ion interactions, and $\underset{\sim}{P}$ is the total

electric dipole moment. By using appropriate exciton and magnon wave functions, we can reduce this moment to the form

$$\underset{\sim}{M} = \sum_{n=1}^{N} e^{i\underset{\sim}{k} \cdot \underset{\sim}{\delta}_{01,n2}} \langle e_{01}\, m_{n2} | \underset{\sim}{P}^{eff}_{01,n2} | \wp g_{01} g_{n2} \rangle \quad . \quad (3)$$

In these expressions $|e\rangle$, $|g\rangle$ and $|m\rangle$ are single-ion wave functions; $g_{01}$ is the ground state of an ion at the $0^{th}$ site on one sublattice, $e_{01}$ is the excited $|^4T_1, 3/2\rangle$ state at the same site and $m_{n2}$ is a $M_s = 3/2$ spin state of the ground state multiplet for an ion at the $n^{th}$ site on the opposite sublattice; $\underset{\sim}{P}^{eff}_{01,n2}$ is the effective dipole moment connecting ions 01 and n2 and results from a combination of V and $\underset{\sim}{P}$ terms of Eq. (2); $\underset{\sim}{\delta}_{01,n2}$ is the vector from site 01 to n2, and $\wp$ is a permutation operator which leads to both direct and exchange terms.

By considering the symmetry of this effective dipole moment under all the operations of the magnetic space group, and including only contributions from the eight near neighbor pairs, the components of Eq. (3) can be written as

$$M_z = 4i\, P_2^z \cos\left(\frac{k_z c}{2}\right) \sin \frac{a}{2}(k_x + k_y)$$

$$M^{\xi} = 4i \sin\left(\frac{k_z c}{2}\right)\left[P_1^{\xi} \cos\frac{a}{2}(k_x - k_y) + P_2^{\xi} \cos\frac{a}{2}(k_x + k_y)\right]$$

$$M^{\eta} = 0 \quad , \quad (4)$$

where $\hat{\xi} = \frac{1}{\sqrt{2}}(\hat{x} + \hat{y})$ and $\eta = \frac{1}{\sqrt{2}}(\hat{y} - \hat{x})$ . Equations (4) are for an exciton on one sublattice. For an exciton on the other sublattice the roles of $M^{\xi}$ and $M^{\eta}$ are reversed. This rather unusual type of coupling is observed for the $\sigma$ sidebands when stress is applied along the $\hat{\xi}$ and $\hat{\eta}$ axes ([110] direction).[9] We see that the form of Eq. (4) gives the selection rules predicted by group theory as it must.

By considering the interaction explicitly we have gained some additional information. We can show that only exchange terms contribute to the process and that the exciton and magnon must be on opposite sublattices. We can see this by considering the spin part of Eq. (3):

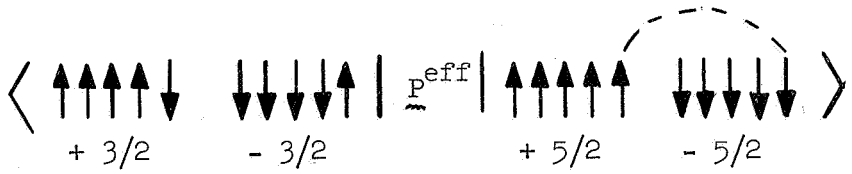


(5)

Since $\underset{\sim}{P}^{eff}$ is spin independent, spin orthogonality will only allow the exchange term (the dotted line schematically indicates the two electrons to be interchanged). The $S_z$ components indicated below the matrix element show that the total $S_z$ of the system is conserved in the transition. It can also be seen from Eq. (3) that spin orthogonality will not allow direct or exchange terms when the exciton and magnon are on the same sublattice. In this case $\Delta S_z = 2$ for the system. This would require higher order processes.

## III. FLUORESCENCE

The sharp line fluorescence in $MnF_2$ at $4.2^oK$ is shown in Fig. 2. We distinguish two regions (A and B) because of their different properties. The lines within each region have similar properties. We have discussed some features of the emission previously[10,11] and have shown that lines 1E and 6E are most likely pure electronic transitions. Lines 3E and 8E have properties which suggest they are magnon sidebands of 1E and 6E . We also briefly discussed the results of fluorescent lifetime studies.[11] In this section we present the results of additional studies as well as more details on the lifetime work. A simple model is proposed which explains many of the gross features of the emission. The experimental results which led to this model will be discussed first.

The sharp lines appear to be caused by impurities. The evidence for this is based on a study of many nominally pure samples obtained from five different crystal growing facilities. We find that the relative intensity of the lines varies from sample to sample and that extra lines appear in some of the samples. These are indicated by the dashed lines in Fig. 2. The same extra lines also appear in the fluorescent spectrum of zinc doped $MnF_2$ , shown qualitatively in Fig. 3. We see that as the zinc concentration increases the extra lines appear and soon dominate the spectrum. Similar impurity dependent fluorescence has been observed by Dietz et al., in both $MnF_2$ [12] and other magnetic crystals.[13]

The fluorescence also exhibits a somewhat anomolous temperature dependent intensity and lifetime. Region A decreases in intensity (as the temperature increases) and disappears around $10^{\circ}K$ . Region B first increases in intensity and then disappears around $35^{\circ}K$. The integrated intensity of the fluorescence (including the broad band to the red of the sharp lines in Fig. 2) decreases abruptly between $4^{\circ}K$ and $10^{\circ}K$ . The lifetime of all the lines studied (1E , 2E , 3E , 6E , 8E) has the exponential form

$$\frac{1}{\tau} = C\, e^{-\Delta/kT} \quad . \tag{6}$$

For lines 1E and 3E $\Delta$ is $76 \pm 5\ cm^{-1}$ . Line 2E has the same lifetime behavior as 1E above $5^{\circ}K$ but has a different behavior below $5^{\circ}K$ . Lines 6E and 8E were difficult to analyze because of background fluorescence and we can only estimate that $\Delta$ is somewhere between 200 and 350 $cm^{-1}$ . As the lifetime becomes shorter, the fluorescent intensity decreases in a similar manner. This is not surprising since they both depend on the population of the fluorescing level.

The fluorescence was also studied with uniaxial stress applied along the [001] and [110] directions. Stress along [001] shifts all the lines linearly to the red by the same amount ( $10 \pm 1\ cm^{-1}$ for a stress of $800\ kg/cm^2$ ). The shift is the same as that exhibited by the absorption line E1 as was pointed out by Dietz et al.[14] Stress along [110] lifts the sublattice degeneracy and as expected all the lines split into two components. The lines 2E , 3E , 7E and 8E have one component

appear with $\underset{\sim}{\mathcal{E}} \perp [001]$ , $\underset{\sim}{k} \parallel [110]$ . The other component appears with $\underset{\sim}{\mathcal{E}} \parallel [001]$ , $\underset{\sim}{\mathcal{E}} \perp S$ , $\underset{\sim}{k} \parallel [001]$ . A similar behavior was observed for the $\sigma$ polarized absorption sidebands.[9] In addition intensity changes of the lines with stress are observed but these will not be discussed here.

The model which we propose to explain these results is illustrated schematically in Fig. 4. In essence we assume the fluorescence originates from manganese ions in localized sites whose energy levels lie below the exciton absorption line E1 . Ions in these levels may be thermally activated to the exciton band from which the energy is either non-radiatively quenched or transferred to other lower energy impurity levels which can fluoresce. The emitting ions are probably those whose local environment has been changed by an impurity or other defect such that the E1 exciton becomes trapped at a particular site. This model is supported by the recent experiments of Johnson, Dietz and Guggenheim.[15] They have shown that the E1 exciton can efficiently transfer energy to lower lying $Ni^{2+}$ levels even for $Ni^{2+}$ concentrations as low as 15 ppm. Our intensity results indicate there is also transfer to the system causing line 6E .

The lifetime behavior is easily explained by this model. For instance level 1E will have both a radiative and nonradiative contribution to the observed lifetime,

$$\frac{1}{\tau} = \frac{1}{\tau_R} + \frac{1}{\tau_{NR}} \quad . \tag{7}$$

For an activation type process we expect (for $kT < \Delta$ )

$$\frac{1}{\tau_{NR}} = C\, e^{-\Delta/kT} \quad , \qquad (8)$$

where $\Delta$ is the difference in energy between 1E and E1 . This is just what we observe as is shown in Fig. 5. The lifetime at $1.8^{o}K$ ( $35 \pm 1$ msec ) is taken to be the temperature independent radiative lifetime.

Although the broad features of the fluorescence are explained by this model the exact nature and origin of all the lines is still not absolutely determined. The identification of 1E and 6E as pure transitions is quite convincing. Both lines show some magnetic dipole character and split like E1 in an external magnetic field. The lines 2E , 3E , 7E and 8E have properties which suggest they are magnon sidebands. Since the emission appears to be a localized impurity induced phenomena, the excited states will have no dispersion. Therefore, the shape and position of the sidebands should follow only the magnon density of states (Fig. 1). Lines $7_E$ and 8E have this shape and can be associated with the two critical points in the density of states. Line 3E has the appropriate shape but its separation from 1E($46\ cm^{-1}$) or 0E($72\ cm^{-1}$) does not correspond to any critical point. It is possible that 3E is associated with a local magnon mode. The line 2E may be a mode of this type with 0E as its associated pure transition. The stress results also suggest that 2E , 3E , 7E and 8E are magnon sidebands. Their behavior under [110] stress can be shown to be a general characteristic of $\sigma$ sidebands associated with the $^4T_1$ level.[3]

Now what can be said about magnon sidebands in fluorescence? We expect the sideband selection rules to be less restrictive than in absorption since the local site symmetry of the emitting ion is the controlling factor. In principle the selection rules can be found by the methods employed for analyzing the vibronic spectra of impurity ions in crystals.[16] Unfortunately this requires a knowledge of the site symmetry and at present this is not known.

We can, however, obtain some information from the formalism developed for absorption. In particular the interaction can be treated in exactly the same way by using a localized excited state wave function. The transition moment then has the form

$$\underset{\sim}{M} = \sum_{n=1}^{N} e^{i\underset{\sim}{k} \cdot \underset{\sim}{\delta}_{01,nl}} \langle g_{01}\, m_{nl} | \underset{\sim}{P}^{eff}_{01,nl} | \rho e_{01} g_{nl} \rangle \quad . \qquad (9)$$

As in absorption we consider just the spin parts of the matrix element:

$$\left\langle \uparrow\uparrow\uparrow\uparrow\uparrow \;\; \uparrow\uparrow\uparrow\uparrow\downarrow \right| \underset{\sim}{P}^{eff} \left| \uparrow\uparrow\uparrow\uparrow\downarrow \;\; \uparrow\uparrow\uparrow\uparrow\uparrow \right\rangle \qquad (10)$$

$$5/2 \qquad 3/2 \qquad\qquad 3/2 \qquad 5/2$$

Here we see by spin orthogonality that the exchange term contributes for the excited state and magnon on the same sublattice. Both direct and exchange terms are small for the excited state and magnon on opposite sublattices. This simple fact explains the previously puzzling result

that the magnon sidebands do not split in a 10 kOe external magnetic field. In fact, Imbusch[17] has recently shown that the sidebands do not split in external fields up to the critical field (95 kOe) . The explanation for this is analogous to the one given for the absorption sidebands.[10]

## REFERENCES


1. R. L. Greene, D. D. Sell, W. M. Yen, A. L. Schawlow, and R. M. White, Phys. Rev. Letters 15, 656 (1965).
2. J. W. Halley and I. Silvera, Phys. Rev. Letters 15, 654 (1965).
3. D. D. Sell, R. L. Greene and R. M. White, to be published in Physical Review.
4. J. O. Dimmock and R. G. Wheeler, Phys. Rev. 127, 391 (1962).
5. M. Lax and J. J. Hopfield, Phys. Rev. 124, 115 (1961).
6. Similar results have been obtained by Y. Tanabe and K. Gondaira, p. , this volume.
7. S. J. Allen, R. Loudon, and P. L. Richards, Phys. Rev. Letters 16, 463 (1966).
8. Y. Tanabe, T. Moriya, and S. Sugano, Phys. Rev. Letters 15, 1023 (1965).
9. R. E. Dietz, A. Misetich, and H. J. Guggenheim, Phys. Rev. Letters 16, 841 (1966).
10. D. D. Sell, R. L. Greene, W. M. Yen, A. L. Schawlow, and R. M. White, J. Appl. Phys. 37, 1229 (1966).
11. D. D. Sell, R. L. Greene, and A. L. Schawlow, Bull. Am. Phys. Soc. 11, 243 (1966).
12. R. E. Dietz, H. J. Guggenheim, and A. Misetich, p. , this volume.

13. R. E. Dietz, L. F. Johnson, and H. J. Guggenheim in Physics of Quantum Electronics, edited by P. L. Kelley, B. Lax and P. E. Tannenwald (McGraw-Hill Book Company, Inc., New York, 1966).

14. R. E. Dietz, A. Misetich, L. F. Johnson, and H. J. Guggenheim, Bull. Am. Phys. Soc. 11 243 (1966).

15. L. F. Johnson, R. E. Dietz, and H. J. Guggenheim, Phys. Rev. Letters 17, 13 (1966).

16. R. Loudon, Proc. Phys. Soc. (London) 84, 379 (1964).

17. G. F. Imbusch (private communication).

## FIGURE CAPTIONS

1. Brillouin zone and relevant portion of magnon density of states in $MnF_2$ . The density of states is based on the magnon dispersion used in Ref. 7 using exchange and anisotropy constants $J_1 = 0.22\ cm^{-1}$ , $J_2 = -1.22\ cm^{-1}$ , $J_3 = 0$ , and $H_A = 0.737\ cm^{-1}$ .
2. Sharp line structure of $^4T_{1g} \rightarrow {}^6A_{1g}$ $Mn^{2+}$ fluorescence in $MnF_2$ at $4.2^oK$ . Dashed lines appear in some of the samples studied. Solid lines appear in all of the samples.
3. Sharp line $Mn^{2+}$ fluorescence observed in region A for various $Zn^{2+}$ doped $MnF_2$ samples. Extra lines which appear as Zn concentration increases are indicated by arrows. These lines correspond to the dashed lines in Fig. 2.
4. Schematic representation of a model which explains gross features of the fluorescence. (See text.)
5. Fluorescent lifetime of lines in region A as a function of inverse temperature. The corrected lifetime is $\tau_{NR}$ (see text).

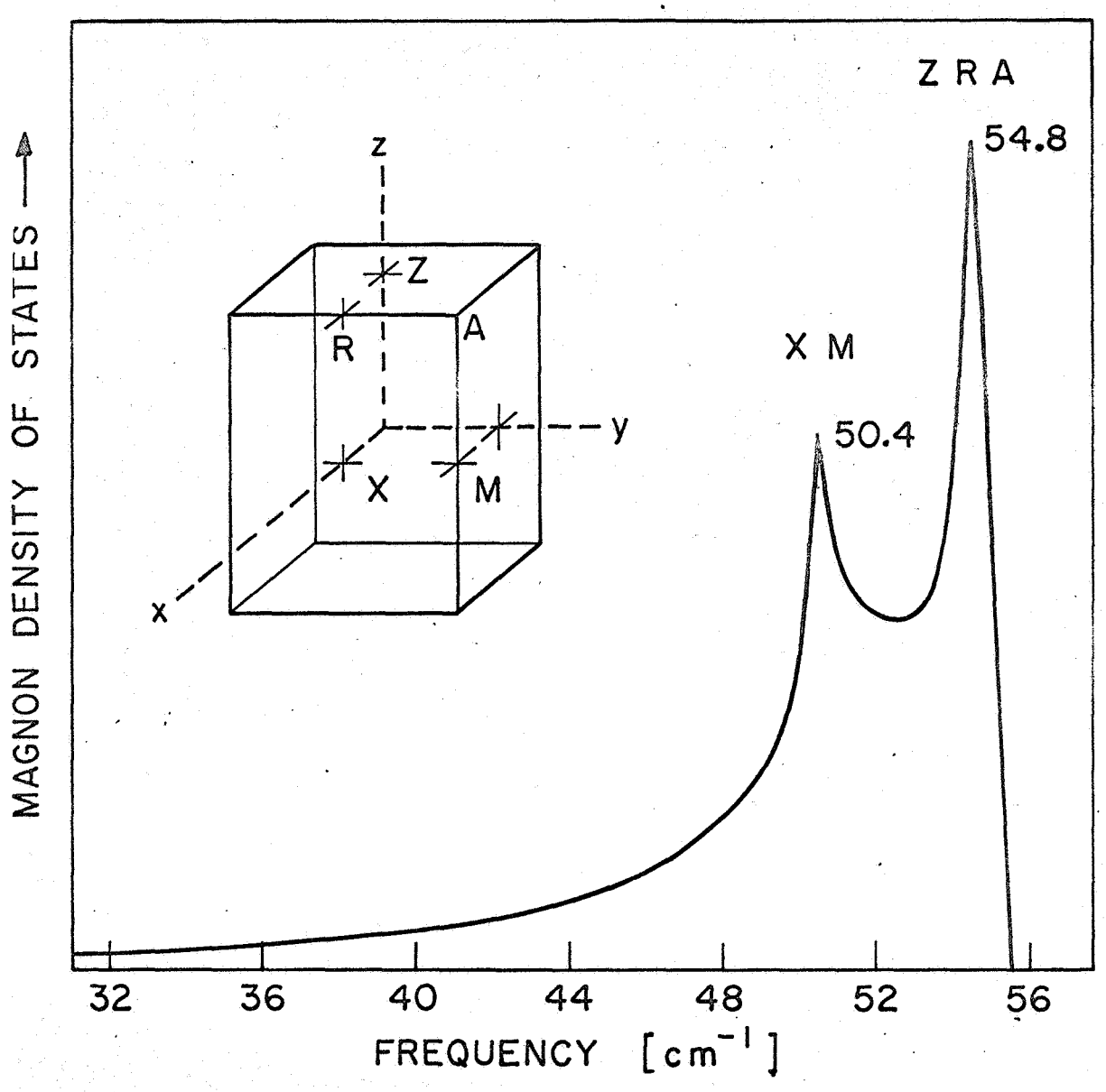
Z R A
54.8
z
Z
R
A
X M
y
50.4
X
M
x
MAGNON DENSITY OF STATES
32
36
40
44
48
52
56
FREQUENCY [cm⁻¹]

FIGURE 1

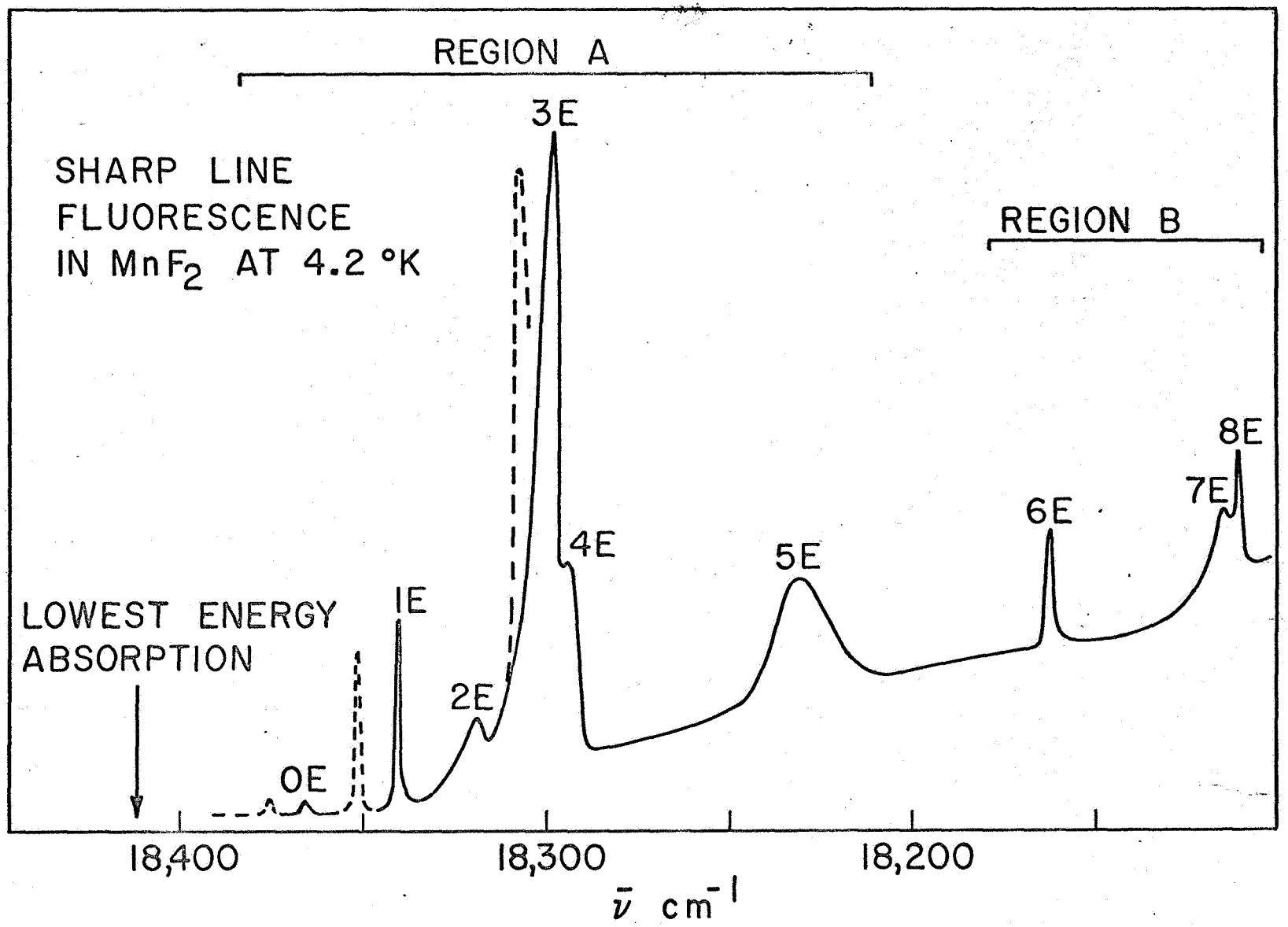
REGION A
3E
SHARP LINE
FLUORESCENCE
IN $MnF_2$ AT 4.2 °K
REGION B
8E
7E
6E
4E
5E
LOWEST ENERGY
ABSORPTION
1E
2E
0E
18,400
18,300
18,200
$\bar{\nu}$ cm$^{-1}$

FIGURE 2

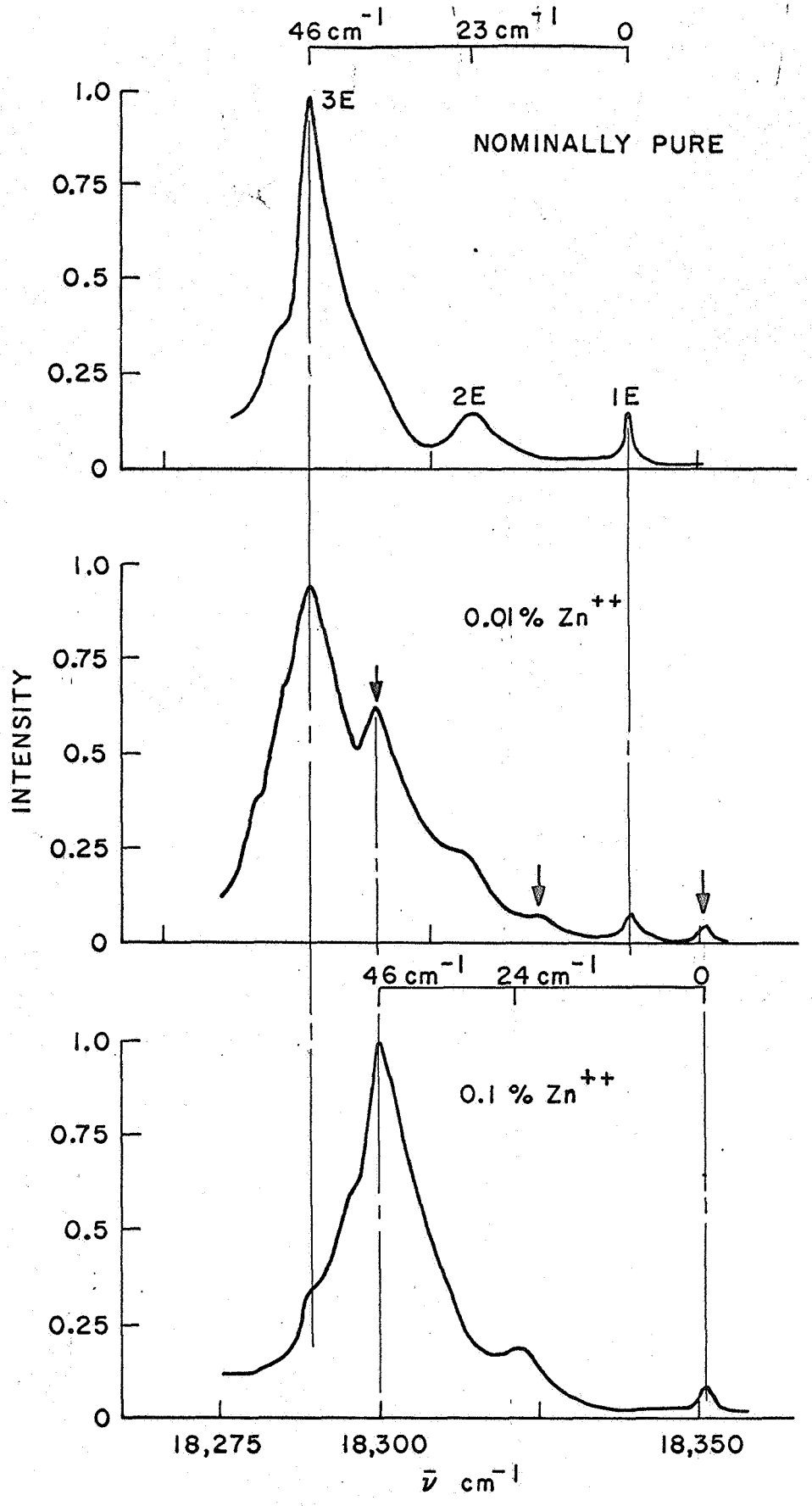
46 cm⁻¹
23 cm⁻¹
0
3E
NOMINALLY PURE
2E
1E
1.0
0.75
0.5
0.25
0
0.01% Zn⁺⁺
INTENSITY
46 cm⁻¹
24 cm⁻¹
0
0.1 % Zn⁺⁺
18,275
18,300
18,350
ν̄ cm⁻¹

FIGURE 3

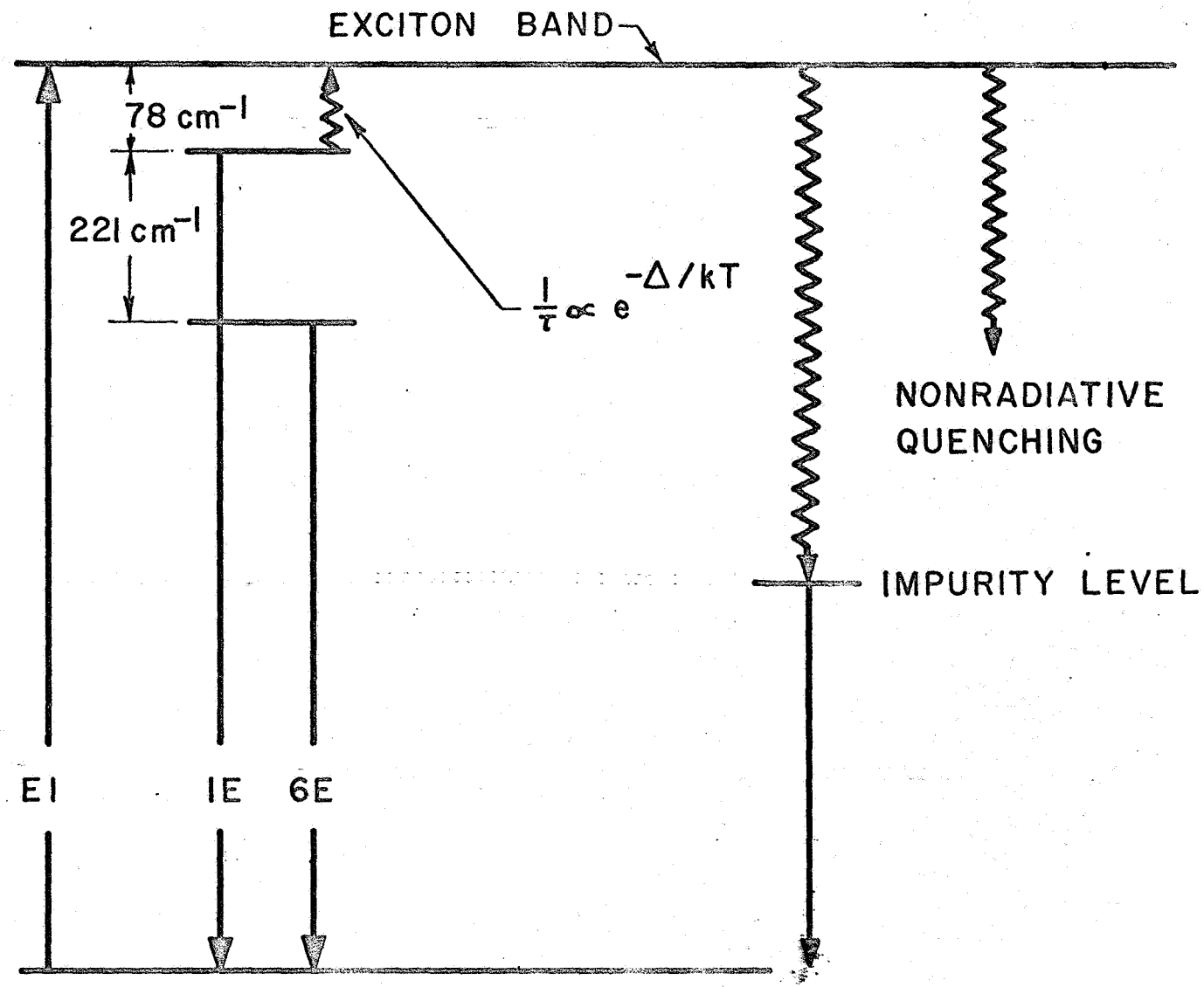
EXCITON BAND
78 cm⁻¹
221 cm⁻¹
$\frac{1}{\tau} \propto e^{-\Delta/kT}$
NONRADIATIVE
QUENCHING
IMPURITY LEVEL
E1
1E
6E

FIGURE 4

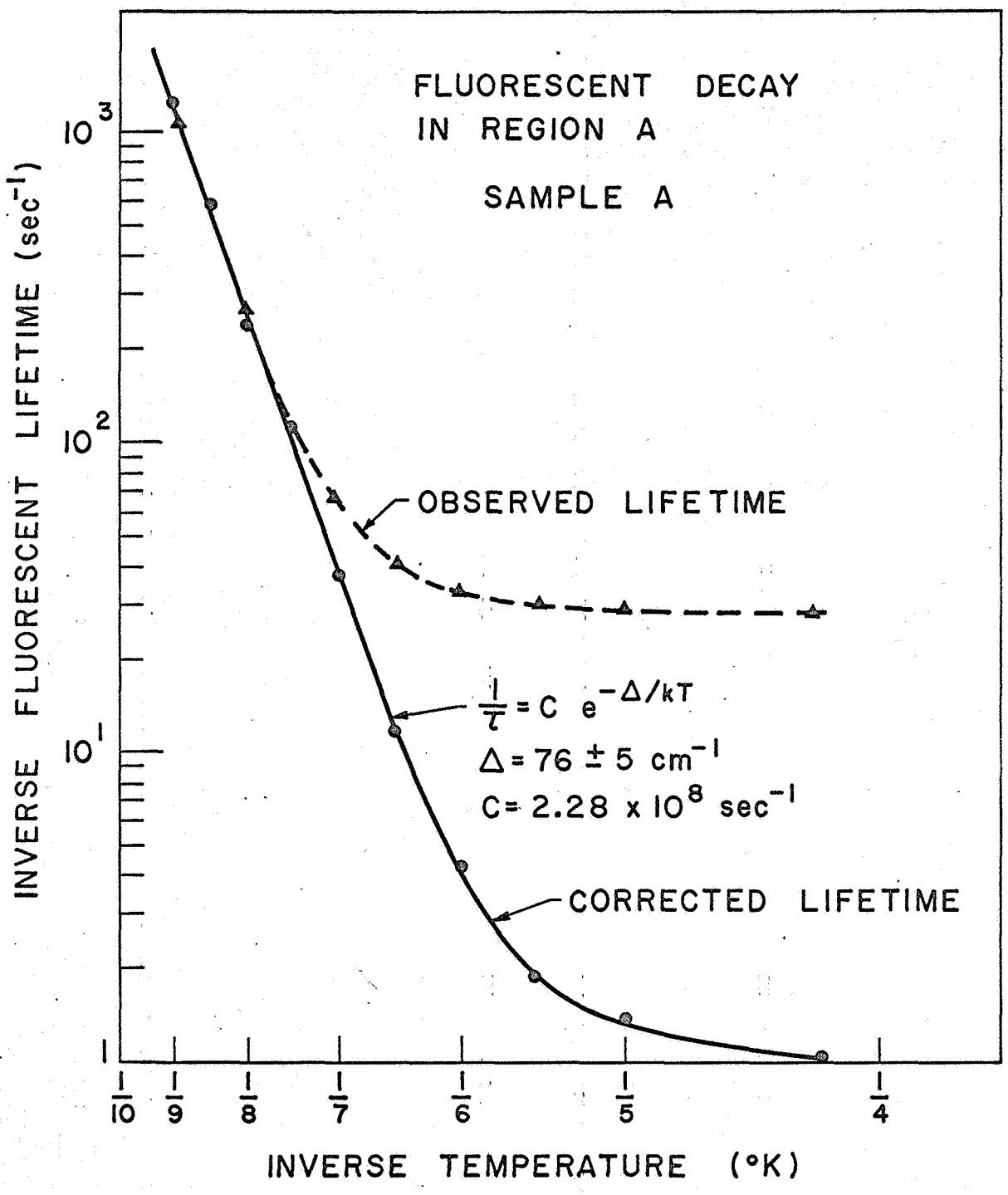
FLUORESCENT DECAY
IN REGION A
SAMPLE A
OBSERVED LIFETIME
$\frac{1}{\tau} = C\ e^{-\Delta/kT}$
$\Delta = 76 \pm 5\ cm^{-1}$
$C = 2.28 \times 10^{8}\ sec^{-1}$
CORRECTED LIFETIME
INVERSE FLUORESCENT LIFETIME ($sec^{-1}$)
$10^3$
$10^2$
$10^1$
1
$\frac{1}{10}$ $\frac{1}{9}$ $\frac{1}{8}$ $\frac{1}{7}$ $\frac{1}{6}$ $\frac{1}{5}$ $\frac{1}{4}$
INVERSE TEMPERATURE (°K)

FIGURE 5